Journal of Nanostructure in Chemistry (2020) 10:97–103
https://doi.org/10.1007/s40097-020-00332-2

ORIGINAL RESEARCH

Characterization of nanocrystalline nickel oxide thin films prepared at different thermal oxidation temperatures

Fatemeh Hajakbari[1]

Received: 19 July 2019 / Accepted: 22 January 2020 / Published online: 3 February 2020

Abstract

Nickel oxide (NiO) thin films were obtained by thermal oxidation of nickel layers coated on quartz. The influence of thermal oxidation temperatures on chemical and physical properties of prepared films was studied. X-ray results exhibited that all the films possess single cubic crystal structure phase of NiO along the (200) plane, and show good crystalline quality. The crystallinity of NiO films is increased with increase in oxidation temperature. Also, the structural parameters of the films were determined. The mean crystallite size was varied between 17 and 45 nm, which confirms the formation of nanocrystals in this study. Also, FTIR and EDS studies confirm the formation of NiO. According to SEM and AFM images, the grain size was influenced by augmentation in thermal oxidation temperature. The optical studies showed that with increase in thermal oxidation temperature, the transmittance increased, while the optical band gap decreased.

Graphic abstract

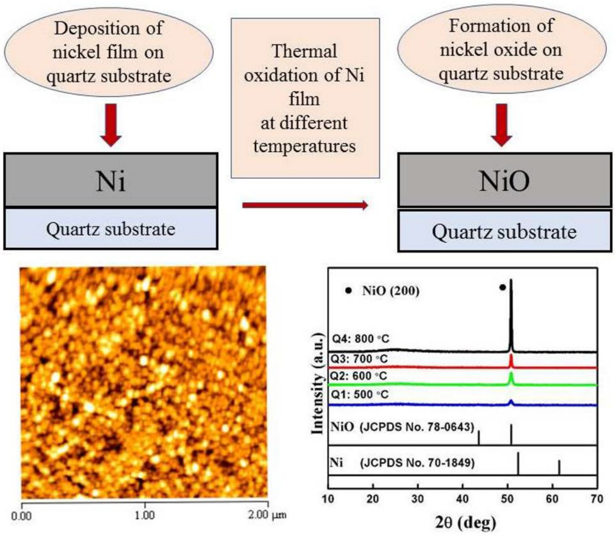

Keywords NiO · Nanocrystalline · Thermal oxidation · Thin film · Sputtering

Introduction

Metal oxide nanostructures with narrow and large band gap have been widely investigated for their potential applications in various fields [1–5]. Among these, nanostructure nickel oxides have recently attracted considerable attention owing

---

✉ Fatemeh Hajakbari
Fatemeh.hajakbari@kiau.ac.ir

[1] Department of Physics, Karaj Branch, Islamic Azad University, Karaj, Iran

to their unique chemical, electrical, and optical properties [6–10]. The most attractive properties of NiO thin films are excellent durability, electrochemical stability, low material cost, semi-transparent p-type semiconductor, stable direct wide optical band gap, and possibility of producing using different techniques for various applications [11–15]. NiO films have been widely applied in gas sensor [1], chemical sensors [2], solar cell [7], and electrochromic devices [10]. Several chemical and physical techniques were applied to deposit NiO films on various substrates [16–19]. Spray pyrolysis, spin coating, metal organic chemical vapor deposition, electron beam evaporation, magnetron sputtering, sol–gel, and thermal oxidation have been the most preparation methods of NiO films. Also, the plasma oxidation of nickel layers is an alternative method to prepare NiO films [20, 21]. Thermal oxidation of metal thin films is very low cost and simple way of synthesis of metal oxide films [14, 15, 22]. Furthermore, the deposition technique and parameters can influence on properties and application of thin films [23–28]. Therefore, in the present work, thin stoichiometric NiO films were obtained by two-step method. First, nickel layers were coated on quartz using direct current (DC) magnetron sputtering. Then, thermal oxidation of Ni films was employed to prepare NiO films. In the previous work [14], we have used thermal oxidation of nickel films in temperature of 400–600 °C to study the properties of fabricated NiO films. Here, we report the influence of thermal oxidation temperature up to 800 °C on physical and chemical properties of the nickel oxide films. Also, the initial nickel layer thickness in this work is 100 nm, while the Ni thickness in previous work was 50 nm. The obtained results show that the initial nickel layer thickness and thermal oxidation temperature influence the structural, morphological, and optical properties of the prepared nickel oxide films.

Experimental details

In this experiment, first, pure nickel (Ni) thin films were deposited onto quartz substrates by DC magnetron sputtering of Ni (99.999%) target using argon (99.99%) gas. The pre-sputtering of target was done for about 10 min to clean the oxide layers on the surface of target. The substrates were pre-cleaned in an ultrasonic bath to prevent impurity before starting deposition process. The sputtering of Ni was done at ambient temperature in an argon atmosphere. Deposition parameters for sputtering of Ni thin films are summarized in Table 1. After deposition, all the as-deposited Ni films were thermally treated in oxygen atmosphere in electrical furnace at different temperatures of 500, 600, 700, and 800 °C for 240 min duration. The samples prepared at different temperatures were named as Q1, Q2, Q3, and Q4, respectively.

Table 1 Deposition parameters of Ni films

Parameters	Values
Base pressure (mbar)	5.8×10^{-5}
Deposition pressure (mbar)	7×10^{-3}
Sputtering gas (99/99%)	Ar
Target (99/999%)	Ni
Target-to-substrate distance (cm)	4.2
Deposition time (min)	40
Voltage (V)	160
Current (A)	0.20

Table 2 Structural parameters, roughness, and E_g values of NiO films

Thermal oxidation temperature (°C)	500	600	700	800
Crystallite size (nm)	17	21	41	45
Microstrain ε ($\times10^{-3}$)	5.30	4.30	2.20	2.00
Dislocation density δ ($\times10^{15}$ Lines/m^2)	3.20	2.10	0.58	0.47
Film thickness (nm)	75	80	85	91
RMS roughness R_q (nm)	2.65	5.48	8.53	12.62
Average roughness R_a (nm)	2.06	4.23	6.43	9.30
Mean height (nm)	10.92	20.10	55.23	65.54
E_g (eV)	3.60	3.56	3.50	3.47

The NiO film thickness was measured by Detak3 surface profilometer. The data of films thickness are shown in Table 2. To identify the crystalline structure of prepared films, X-ray diffraction (XRD) measurements were performed using a Philips, pw1800 diffractometer by CoK$_\alpha$ ($\lambda = 0.17890$ nm) radiation in 2θ range from 10° to 70°.

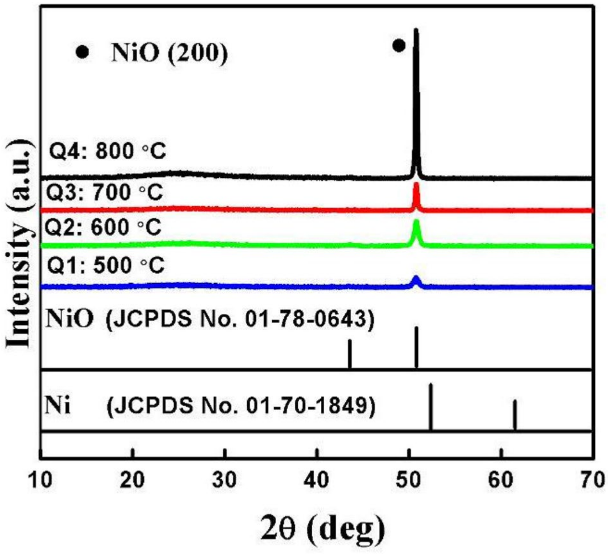

Fig. 1 X-ray diffraction spectra of nickel oxide films

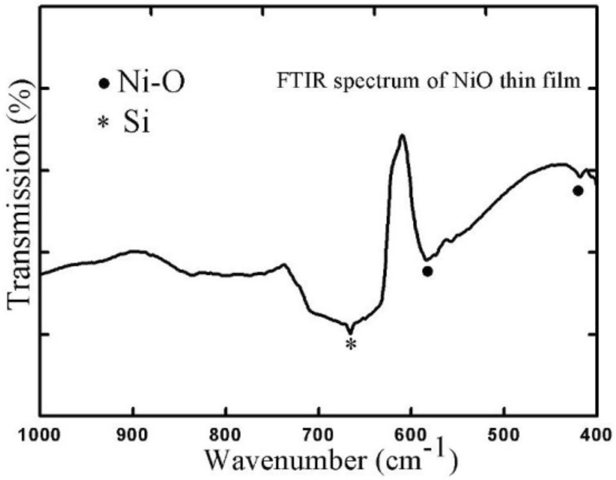

Fig. 2 FTIR spectrum of NiO thin film

Fourier transform infrared (FTIR) spectra of the films in the range of 400–1000 cm^{-1} were recorded using spectrophotometer model Perkin Elmer. The morphology of prepared samples was investigated using scanning electron microscopy (SEM: Hitachi S-4160). The elemental composition of films was obtained by the energy-dispersive spectroscopy (EDS) which attached on the SEM device. Atomic force microscopy (AFM: Park Scientific Instrument, Auto probe cp USA) in contact mode was carried out to study the surface topography and roughness of films. The optical transmittance of the NiO films in the range of 200–1100 nm was recorded by UV–Vis spectrophotometry (CARY 500 Scan).

Results and discussion

Figure 1 depicts the XRD patterns of the samples fabricated at various thermal oxidation temperatures of 500–800 °C. We can observe that all of the samples displayed only one sharp peak at $2\theta = 50.70°$ which belongs to reflection from (200) plane of cubic NiO phase (JCPDS No. 01–78-0643). When the NiO film is directly deposited in amorphous substrates, the (200) diffraction peak of the cubic structure can be observed [16, 23]. In addition, the (200) peaks intensity

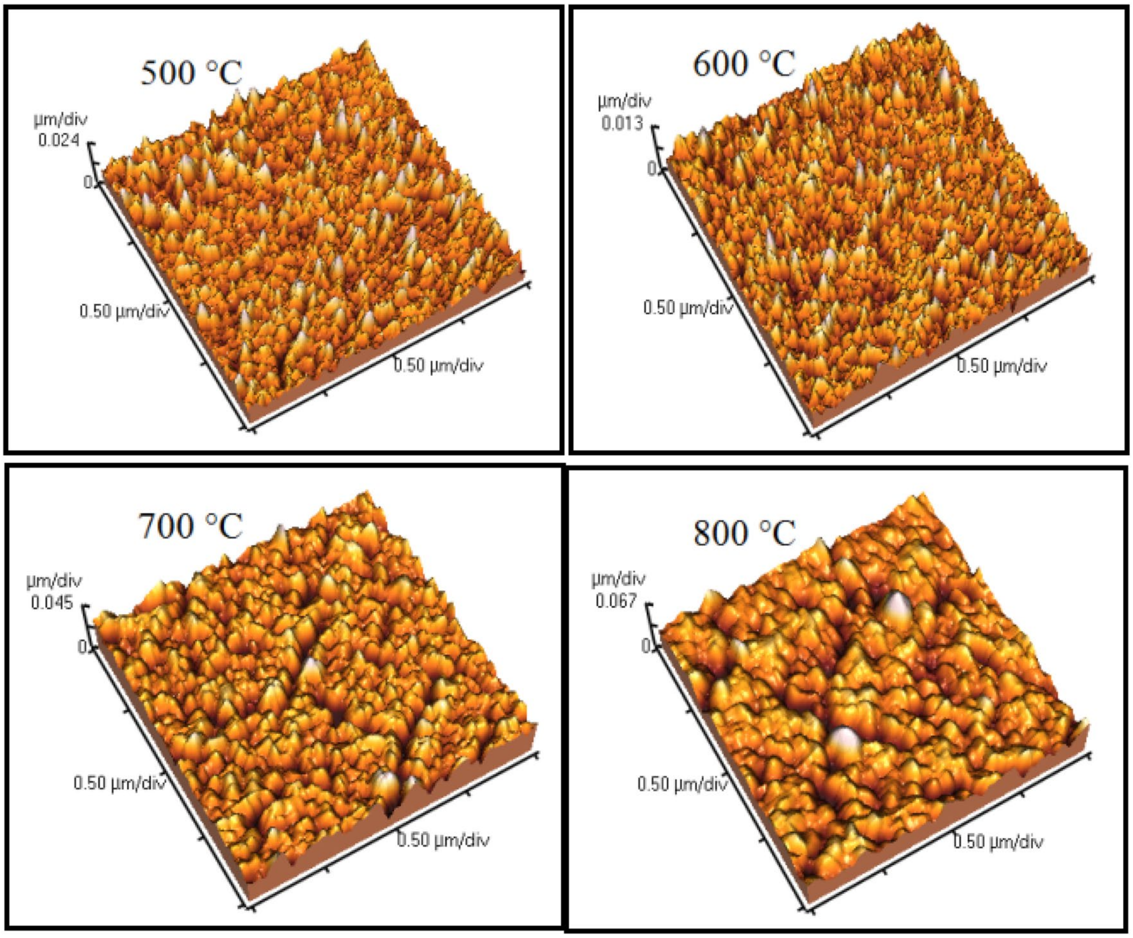

Fig. 3 3D AFM images for NiO films on quartz

also increases with thermal oxidation temperature suggesting an improvement of the films crystallinity [14, 19]. In comparison to our previous work [14], we can observe that higher oxidation temperature of 700 and 800 leads to improvement of film crystallinity. At higher temperature, the atoms of the films can gain more energy and the surface mobility increases and the grain growth promotes; therefore, the crystallinity is improved. The XRD results reveal that no other peak appeared except the NiO peak which approves the creation of single phase of NiO.

A simple estimation of the crystallite sizes of the films was estimated using the Scherrer equation as presented in Eq. (1) [20]:

$$D = 0.9\lambda / \beta \cdot \cos\theta, \tag{1}$$

where D is the crystallite size, λ is the wavelength of X-ray, β is the full width at half maximum (FWHM) value of the diffraction peak, and θ is the Bragg diffraction angle. The microstrain (ε) and dislocation density (δ) of the NiO films were evaluated from Eqs. 2 and 3:

$$\varepsilon = \beta / 4 \tan\theta, \tag{2}$$

$$\delta = 1/D^2, \tag{3}$$

The calculated values of D, ε and δ are presented in Table 2. According to data listed in Table 2, the determined crystallite sizes of the samples are 17, 21, 41, and 45 nm for thermal oxidation temperatures of 500, 600, 700, and 800 °C, respectively. In addition, the crystallite size increase with augmentation of oxidation temperatures may be due to the coalescence of the smaller crystallites and formation of a larger crystallite during the heating process [14, 19].

The microstrain and dislocation density values decrease with increase in oxidation temperatures. The estimated crystallite sizes confirm the formation of nanocrystalline NiO films in this work [6, 14]. Additionally, we can observe that the FWHM of (200) peak and microstrain decreased with enhancement of oxidation temperatures owing to the reduction of dislocation density along grain boundaries with an increase in crystallite size [17]. The XRD results indicate that thermal oxidation temperature has significant effect in improving the film crystallinity.

The FTIR examination employed to approve the formation of NiO films. The silicon substrate is transparent in IR region; therefore, for FTIR analysis, the film deposited on silicon substrate was employed. Typical FTIR spectrum of the film fabricated at temperature of 600 °C in range 400—1000 cm^{-1} is shown in Fig. 2.

The peaks appeared at 418.16 and 580.76 are related to the Ni–O bond of nickel oxide [20]. The peak at 665.20 cm^{-1}

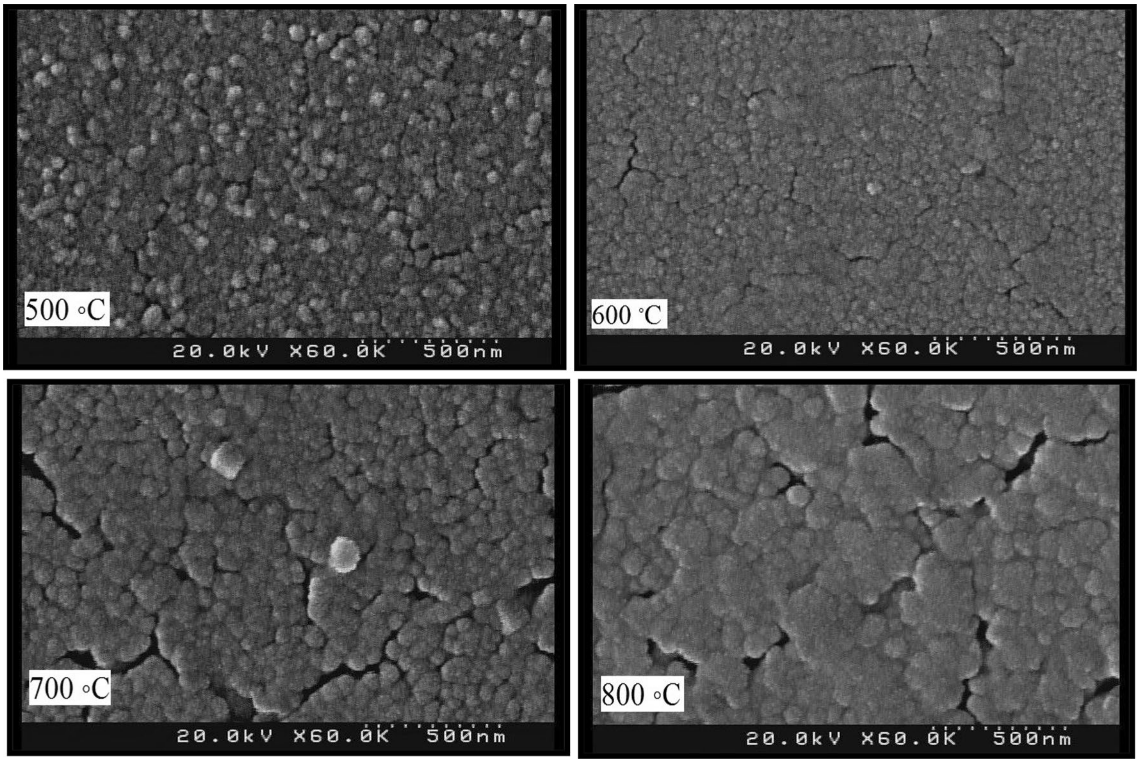

Fig. 4 SEM micrographs of nickel oxide films

belongs to silicon substrate. FTIR results confirm the NiO formation.

Surface topography can influence the properties of thin films. Thus, surface topography of prepared films was studied using AFM. The 3D micrographs for all samples are revealed in Fig. 3. The images showed that the films were composed of well-formed nanoparticles that uniformly distributed over the evaluated films area and confirm the growth of grains and improvement of crystalline microstructure. A few important parameters such as the root-mean-square (RMS) roughness (R_q), the average roughness (R_a), and the mean height [28] were estimated from the AFM measurements and the mentioned parameters values are presented in Table 2. The values of this table show that as thermal oxidation temperature increases from 500 to 800 °C, the above set of parameters gradually increase and exhibits the similar trends. The increase in surface roughness can be due to enhancement of the crystallite size and film thickness [10].

SEM analysis was performed to investigate the morphology of the samples. The top view SEM images of the NiO films fabricated at temperature of 500, 600, 700, and 800 °C are revealed in Fig. 4. These images exhibit a compact distribution of distinct grains with various sizes. The SEM micrographs indicate that the morphology is highly sensitive to oxidation temperature. In addition, an increment in thermal oxidation temperatures leads to creation of cracks and agglomeration of small grains. The crack width increased by oxidation temperatures due to release of strain energy [29]. In comparison to our previous work [14] at higher initial Ni thickness and oxidation temperature, the films' adhesion to the substrate reduces and the films start to crack. Similar behavior was obtained by the other authors [22].

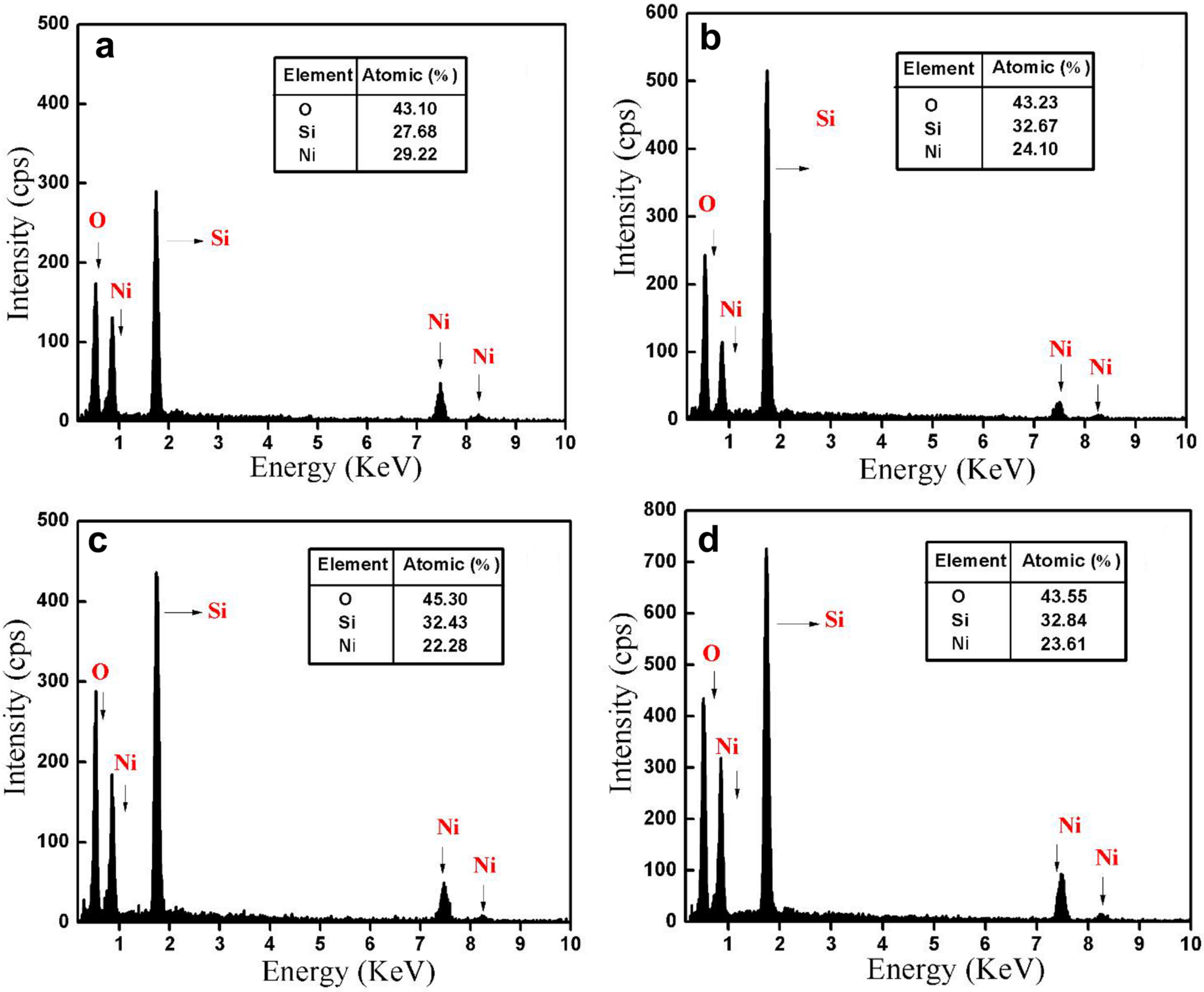

Element	Atomic (%)
O	43.10
Si	27.68
Ni	29.22

Element	Atomic (%)
O	43.23
Si	32.67
Ni	24.10

Element	Atomic (%)
O	45.30
Si	32.43
Ni	22.28

Element	Atomic (%)
O	43.55
Si	32.84
Ni	23.61

Fig. 5 EDS spectra of nickel oxide films prepared at different temperatures: **a** 500, **b** 600, **c** 700, and **d** 800 °C

The elemental composition of films was examined by EDS. Figure 5 exhibits the EDS patterns of NiO films fabricated at various oxidation temperatures. The obtained spectra approve the existence of nickel and oxygen elements in the film. On the other hand, as the oxygen peak in EDS spectrum is belonging to nickel oxide thin film and to the quartz substrate, an exact quantitative analysis is not possible. The peak of Si is due to the quartz substrate. The EDS results confirm the formation of pure nickel oxide films [21].

Figure 6a illustrates the spectral transmittance of films prepared at different oxidation temperatures. Optical transmittance spectra show strong dependence on the oxidation temperature. Furthermore, the transparency of films is increased with elevation of thermal oxidation. This can be due to the change of nickel to nickel oxide, increase in thickness of NiO film, improvement of crystalline microstructure, and less defect scattering. According to Fig. 6b, an augmentation of oxidation temperature causes the absorption edge shifts to smaller wavelengths may be due to enhancement in crystal quality [18]. The NiO thin film optical properties were determined by optical transmittance measurements. The absorption coefficient (α) and optical energy gap (E_g) were determined from the following formulas [30]:

$$\alpha = (1/d)\ln(1/T), \tag{4}$$

$$(\alpha h\nu)^{1/n} = A\left(h\nu - E_g\right), \tag{5}$$

where d, T, and $h\nu$ are the film thickness, transmittance, and photon energy, respectively. A is a constant and n for NiO films with direct band gap energy [4, 14, 18, 20] is equal to 0.5. The plot of $(\alpha h\nu)^2$ against $h\nu$ was employed to estimate the direct energy gaps of the prepared films. According to Fig. 7, the estimated values of E_g for nickel oxide films fabricated at various oxidation temperatures of 500, 600, 700, and 800 °C were in range of 3.47–3.60 eV. These values are in agreement with the values achieved by other workers [4, 14, 18, 20]. Moreover, the optical band gap energy (E_g) values were decreased with an augmentation of oxidation temperature. This can be related to improve the crystallite size with increment of thermal oxidation temperature [18].

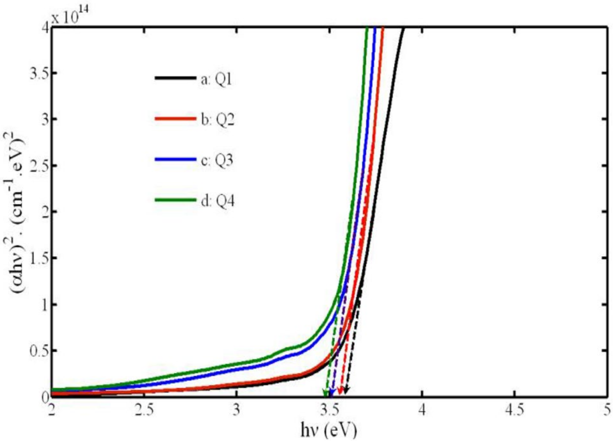

Fig. 7 Plot of $(\alpha h\nu)^2$ versus $(h\nu)$ for nickel oxide films

Conclusion

In conclusion, nanocrystalline NiO thin films were grown through thermal oxidation of Ni layers coated on quartz by DC magnetron sputtering. The XRD measurement indicates the formation of cubic structure of NiO with orientation along

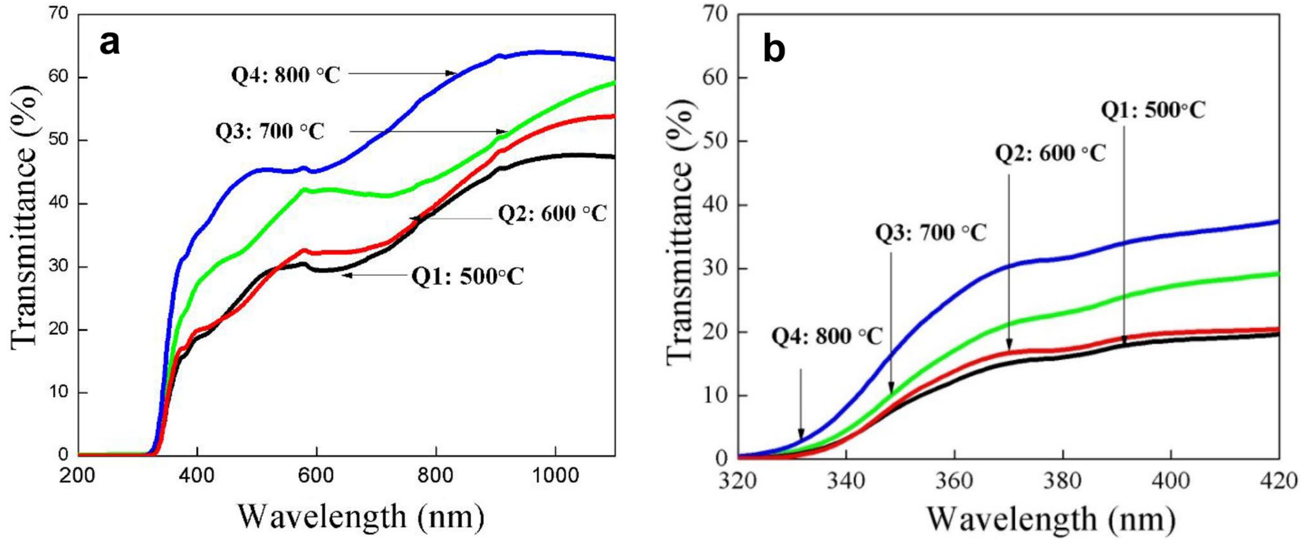

Fig. 6 **a** Transmittance spectra and **b** the shift of absorption edge of NiO samples (Q1, Q2, Q3, and Q4)

(200) plane. The augment in the grain size of the NiO thin films during thermal oxidation was confirmed by the XRD, AFM, and SEM profiles. The band gap energy values reduced from 3.60 to 3.47 eV by augmentation of oxidation temperature owing to enhance crystallinity resulted through decrease of defects during the thermal oxidation. From the results, it is concluded that the thermal oxidation temperatures effectively influenced the characteristic properties of prepared films.

Author contribution statement The design and experiment, the preparation, editing and reviewing of the manuscript have performed by FH.

References

1. Ukoba, K.O., Eloka-Eboka, A.C., Inambao, F.L.: Review of nanostructured NiO thin film deposition using the spray pyrolysis technique. Renew. Sustain. Energy Rev. **82**, 2900–2915 (2018)
2. Saric, I., Peter, R., Kavre, I., Badovinac, I.J., Petravic, M.: Oxidation of nickel surfaces by low energy ion bombardment. Nucl. Instr. Methods Phys. Res. B. **371**, 286–289 (2016)
3. Yueying, L., Fengmin, L., Jihao, B., Tianyu, L., Ziyang, Y., Meng, D., Linsheng, Z., Hongtao, W., Yiqun, Z., Hui, S., Geyu, L.: Direct growth of NiO films on Al_2O_3 ceramics by electrochemical deposition and its excellent H_2S sensing properties. Sens. Actuator B. **296**, 126619 (2019)
4. Kuanr, S.K., Vinothkumar, G., Suresh Babu, K.: Substrate temperature dependent structural orientation of EBPVD deposited NiO films and its influence on optical, electrical property. Mat. Sci. Semicon. Proc. **75**, 26–30 (2018)
5. Zrikem, K., Song, G., Ait Aghzzaf, A., Amjoud, M., Mezzane, D., Rougier, A.: UV treatment for enhanced electrochromic properties of spin coated NiO thin films. Superlattices. Microst. **127**, 35–42 (2019)
6. El-Nahass, M.M., Emam-Ismail, M., El-Hagary, M.: Structural, optical and dispersion energy parameters of nickel oxide nanocrystalline thin films prepared by electron beam deposition. J. Alloys Compd. **646**, 937–945 (2015)
7. Yan, X., Zheng, J., Zheng, L., Lin, G., Lin, H., Chen, G., Du, B., Zhang, F.: Optimization of sputtering NiO_x films for perovskite solar cell application. Mater. Res. Bull. **103**, 150–157 (2018)
8. Chtouki, T., Soumahoro, L., Kulyk, B., Bougharraf, H., Kabouchi, B., Erguig, H., Sahraoui, B.: Comparison of structural, morphological, linear and nonlinear optical properties of NiO thin films elaborated by spin-coating and spray pyrolysis. Optik **128**, 8–13 (2017)
9. Roffi, T.M., Nozaki, S., Uchida, K.: Growth mechanism of single-crystalline NiO thin films grown by metal organic chemical vapor deposition. J. Cryst. Growt. **451**, 57–64 (2016)
10. Pereira, S., Goncalves, A., Correia, N., Pinto, J., Pereira, L., Martins, R., Fortunato, E.: Electrochromic behavior of NiO thin films deposited by e-beam evaporation at room temperature. Sol. Energy Mater. Sol. Cells. **120**, 109–115 (2014)
11. Oh, J.H., Hwang, S.Y., Kim, Y.D., Song, J.H., Seong, T.Y.: Effect of different sputtering gas mixtures on the structural, electrical, and optical properties of p-type NiO thin films. Mat. Sci. Semicon. Proc. **16**, 1346–1351 (2013)
12. Zhou, K., Qi, Z., Zhao, B., Lu, S., Wang, H., Liu, J., Yan, H.: The influence of crystallinity on the electrochromic properties and durability of NiO thin films. Surf. Interface. **6**, 91–97 (2017)
13. Raghavana, L., Ojhaa, S., Sulaniaa, I., Mishrab, N.C., Ranjith, K.M.C., Baenitzc, M., Kanjilal, D.: Thermal annealing induced competition of oxidation and grain growth in nickel thin films. Thin Solid Films **680**, 40–47 (2019)
14. Hajakbari, F., Afzali, M.T., Hojabri, A.: Nanocrystalline nickel oxide (NiO) thin films grown on quartz substrates: influence of annealing temperatures. Acta. Phys. Pol A. **131**(3), 417–419 (2017)
15. Zhang, Y.: Thermal oxidation fabrication of NiO film for optoelectronic devices. Appl. Surf. Sci. **344**, 33–37 (2015)
16. Shaaban, E.R., Kaid, M.A., Ali, M.G.S.: X- ray analysis and optical properties of nickel oxide thin films. J. Alloys Compd. **613**, 324–329 (2014)
17. Khalaf, M.K., Mutlak, R.H., Khudiar, A.I., Hial, Q.G.: Influence of discharge voltage on the sensitivity of the resultant sputtered NiO thin films toward hydrogen gas. Phys. B **514**, 78–84 (2017)
18. Ksapabutr, B., Nimnuan, P., Panapoy, M.: Dense and uniform NiO films fabricated by one-step electrostatic spray deposition. Mater. Lett. **153**, 24–28 (2015)
19. Yang, P., Li, L., Yu, S., Zheng, H., Peng, W.: The annealing temperature and films thickness effect on the surface morphology, preferential orientation and dielectric property of NiO films. Appl. Surf. Sci. **493**, 396–403 (2019)
20. Rashvand, S., Hojabri, A.: Structural, morphological and optical properties of nanostructure nickel oxide thin films grown on quartz substrates by plasma oxidation. J. Inorg. Oregnomet. Polym. **27**, 503–509 (2017)
21. Hajakbari, F., Rashvand, S., Hojabri, A.: Effect of plasma oxidation parameters on physical properties of nanocrystalline nickel oxide thin films grown by two-step method: DC sputtering and plasma oxidation. J. Theor. Appl. Phys. **13**(4), 365–373 (2019)
22. Ravikumar, P., Taparia, D., Alagarsamy, P.: Thickness-dependent thermal oxidation of Ni into NiO thin film. J. Supercond. Nov. Magn. **31**(11), 3761–3775 (2018)
23. Valladares, L.D.L.S., Ionescu, A., Holmes, S., Barnes, C.H.W., Dominguez, A.B., Quispe, O.A., Gonzalez, J.C., Milana, S., Barbone, M., Ferrari, A.C., Ramos, H., Majima, Y.: Characterization of Ni thin films following thermal oxidation in air. J. Vac. Sci. Technol. B **32**(5), 051808 (2014)
24. Battiato, S., Giangregorio, M.M., Catalano, M.R., Lo Nigro, R., Losurdo, M., Malandrino, G.: Morphology-controlled synthesis of NiO films: the role of the precursor and the effect of the substrate nature on film structural/optical properties. RSC Adv. **6**(37), 30813–30823 (2016)
25. Peng, S., Zeng, X., Li, Y.: Titanate nanotube modified with different nickel precursors for enhanced Eosin Y-sensitized photocatalytic hydrogen evolution. Int. J. Hydrogen Energy. **40**, 6038–6049 (2015)
26. Zhang, W., Li, Y., Peng, S.: Template-Free synthesis of hollow Ni/Reduced graphene oxide composite for efficient H_2 evolution. J. Mater. Chem. A. **5**, 13072–13078 (2017)
27. Zhang, W., Li, W., Li, Y., Peng, S., Xu, Z.: One-step synthesis of nickel oxide/nickel carbide/graphene composite for efficient dye-sensitized photocatalytic H_2 evolution. Catal. Today. **335**, 326–332 (2019)
28. Rana, R., Chakraborty, J., Tripathi, S.K., Nasim, M.: Study of conducting ITO thin film deposition on flexible polyimide substrate using spray pyrolysis. J. Nanostruct. Chem. **6**, 65–74 (2016)
29. Kalisz, M., Grobelny, M., Kaczmarek, D., Domaradzki, J., Mazur, M., Wojcieszak, D.: Comparison of structural, mechanical and corrosion properties of TiO_2-WO_3 mixed oxide films deposited on TiAlV surface by electron beam evaporation. Appl. Surf. Sci. **421**, 185–190 (2017)
30. Jalili, S., Hajakbari, F., Hojabri, A.: Effect of silver thickness on structural, optical and morphological properties of nanocrystalline Ag/NiO thin films. J. Theor. Appl. Phys. **12**, 15–22 (2018)